DINAME 2019 - Proceedings of the XVIII International Symposium on Dynamic Problems of Mechanics,
M.A. Savi, T.G. Ritto and W.M. Bessa (Editors), ABCM, Buzios, RJ, Brazil, March 10th to 15th, 2019

Modeling of a double pendulum on a cart using the Gibbs-Appell method and implementing LQR control

Ivan Ekman[1], **Flavius Martins**[1], **Tarcisio Hess**[1], **and Roberto Spinola**[1]

[1] Universidade de São Paulo, Av. Prof. Mello Moraes, 2231 - Cidade Universitária Prédio de Engenharia Mecânica e Mecatrônica

Abstract: The aim is to demonstrate the usefulness of the Gibbs-Appell method for modeling serial mechanisms and robots. Gibbs-Appell equations of motion are used to model a double pendulum on a cart; the model is validated through a series of simulations. An inverse dynamics exercise is presented to illustrate the power of feed-forward based on the dynamics of the system. Finally, LQR is proposed to control the double inverted pendulum.

Keywords: Gibbs-Appell, LQR Control, Feed-Forward, Dynamic Modeling, Planar Mechanism.

INTRODUCTION

The construction of a dynamic model and its subsequent simulation help the design of mechanisms, be it in mechanical sizing or in the analysis of its dynamic behavior. It is also necessary to design a proper control.

There are different ways of obtaining model equations. The Gibbs-Appell method was chosen here since it is more effective when modeling systems with non-holonomic constraints as compared to the Lagrangian method (Desloge, 1988; Wang and Pao, 2003). It also requires fewer parameters than Newton-Euler's method. Even though the proposed mechanism does not have non-holonomic constrains, this method allows more versatility (Matarazzo Orsino and Hess-Coelho, 2015) for the continuity of this project.

Gibbs-Appell Equations of Motion have been used to model a two-wheeled robot (Li et al., 2014). It has a similar working principle as the mechanism proposed here. It is an example of how powerful the method can be. This paper intends to demonstrate the usefulness of the Gibbs-Appell method for modeling serial mechanisms and robots.

MODEL

The first step is to define the model to be studied. The double pendulum on a cart was chosen. To explore the simulation possibilities, we considered motors, torsional springs and dampers attached to both rotation joints. These 3-body and 3 degrees of freedom can be described by 3 generalized coordinates, x, $\gamma_{[1]}$ and $\gamma_{[2]}$. All the system variables and properties are defined in Table 1. Not Applicable (NA) values will be defined depending on the case study.

GIBBS-APPELL EQUATIONS

In this section, the Dynamic equations of the model will be written according to the Gibbs-Appell methodology (Baruh, 1999; Kane and Levinson, 1985).

The Gibbs-Appell Equation is given by:

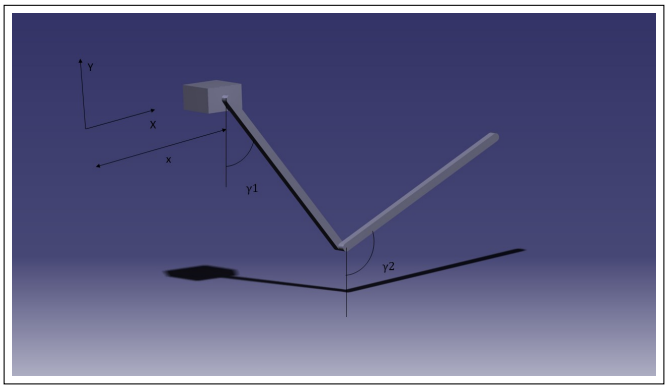

Figure 1: Detailed Model

Table 1: System Variables and Properties

Symbol	Meaning	Value	Unities
g	Gravity	9.98	$[\frac{m}{s^2}]$
ma	Mass of the cart	1	$[kg]$
m1	Mass of the first bar	2	$[kg]$
m2	Mass of the second bar	2	$[kg]$
l1	Length of the first bar	1	$[m]$
l2	Length of the second bar	1	$[m]$
Fk	Force applied on the cart	NA	$[N]$
M1	Motor Torque applied between the cart and the first bar	NA	$[N*m]$
Ml1	Spring and Damper Torque applied between the cart and the first bar	NA	$[N*m]$
M2	Motor Torque applied between the first bar and the second	NA	$[N*m]$
Ml2	Spring and Damper Torque applied between the first bar and the second	NA	$[N*m]$
kl1	Spring constant between the cart and the first bar	NA	$[\frac{N*m}{rad}]$
bl1	Damping coefficient between the cart and the first bar	NA	$[\frac{N*m*s}{rad}]$
kl2	Spring constant between the first bar and the second	NA	$[\frac{N*m}{rad}]$
bl2	Damping coefficient between the first bar and the second	NA	$[\frac{N*m*s}{rad}]$
Fex	Force Applied on the x_0 direction on the end effector	NA	$[N]$
Fey	Force Applied on the y_0 direction on the end effector	NA	$[N]$
Me	Torque applied on the end effector	NA	$[N*m]$

$$\sum_{i=1}^{N}(v_{G_i}^k * m_i * a_{G_i} + w_i^k * H'_{G_i}) = \sum_{i=1}^{N}(v_{G_i}^k * F_i + w_i^k * M_{G_i}) | k = 1,2,...,n \tag{1}$$

For the double pendulum on a cart, we have $N = 3$ bodies and $k = 3$ degrees of freedom. To complete the equation, we must first obtain:

- Partial velocities of the center of mass - $v_{G_i}^k$ and w_i^k
- Acceleration of the center of mass - a_{G_i}
- Derivative of the angular momentum - H'_{G_i}
- The equivalent external actuation on the center of mass - F_i and M_{G_i}

Velocities and Partial Velocities

The points of interest are:

- A - Center of mass of the cart;
- CM1 - Center of mass of the first bar;
- CM2 - Center of mass of the second bar;

Table 2: Partial Velocities

Velocities \Generalized Velocities	$\dot{x}$ **k=1**	$\dot{\gamma}_{[1]}$ **k=2**	$\dot{\gamma}_{[2]}$ **k=3**
v_A	1(i)	0	0
v_{CM1}	1(i)	$\frac{l1}{2}cos(\gamma_{[1]})(i)+\frac{l1}{2}sin(\gamma_{[1]})(j)$	0
v_{CM2}	1(i)	$l1cos(\gamma_{[1]})(i)+l1sin(\gamma_{[1]})(j)$	$\frac{l2}{2}cos(\gamma_{[2]})(i)+\frac{l2}{2}sin(\gamma_{[2]})(j)$
w_{CM1}	0	1(k)	0
w_{CM2}	0	0	1(k)

Considering the coordinates '0' presented in the model section, velocities are:

$$v_A = \dot{x}(i) + 0(j) \tag{2}$$

The velocity for the center of mass of the first bar can be obtained by using:

$$\begin{aligned} \vec{v}_{CM1} &= \vec{v}_A + \vec{w} \times \vec{r}_A^{CM1} \\ v_{CM1} &= (\dot{x} + \dot{\gamma}_{[1]}\frac{l1}{2}cos(\gamma_{[1]}))(i) + (\dot{\gamma}_{[1]}\frac{l1}{2}sin(\gamma_{[1]}))(j) \end{aligned} \tag{3}$$

The same can be done for CM2. Observe that the center of rotation for the second bar is at the end of the first one (point B); thus:

$$\vec{v}_{CM2} = \vec{v}_B + \vec{w} \times \vec{r}_B^{CM2}$$

$$v_B = (\dot{x} + \dot{\gamma}_{[1]}l1cos(\gamma_{[1]}))(i) + (\dot{\gamma}_{[1]}l1sin(\gamma_{[1]}))(j)$$

Resulting in:

$$v_{CM2} = (\dot{x} + \dot{\gamma}_{[1]}l1cos(\gamma_{[1]}) + \dot{\gamma}_{[2]}\frac{l2}{2}cos(\gamma_{[2]}))(i) + (\dot{\gamma}_{[1]}l1sin(\gamma_{[1]}) + \dot{\gamma}_{[2]}\frac{l2}{2}sin(\gamma_{[2]}))(j) \tag{4}$$

Angular velocities are:

$$w_A = 0(k) \tag{5}$$

$$w_{CM1} = \dot{\gamma}_{[1]}(k) \tag{6}$$

$$w_{CM1} = \dot{\gamma}_{[2]}(k) \tag{7}$$

Partial velocities are defined as:

$$v_{G_i}^k = \frac{\delta v_{G_i}}{\delta u_k} \tag{8}$$

$$w_i^k = \frac{\delta w_i}{\delta u_k} \tag{9}$$

The derivatives are calculated, resulting in the partial velocities shown in Table 2.

Accelerations

Accelerations can be calculated by using:

$$\vec{a} = \vec{a}_G + \vec{\alpha} \times \vec{\rho} + \vec{\omega} \times (\vec{\omega} \times \vec{\rho}) \tag{10}$$

Starting from A:

$$a_A = \ddot{x}(i) \tag{11}$$

Then, following the same steps used to calculate the velocities, $A \longrightarrow CM1 \longrightarrow B \longrightarrow CM2$, we have:

$$\begin{aligned} a_{CM1} = (\ddot{x} + \ddot{\gamma}_{[1]} l1/2 * cos(\gamma_{[1]}) + \dot{\gamma}^2_{[1]} l1/2 * (-sin(\gamma_{[1]})))(i) + \\ +(+\ddot{\gamma}_{[1]} l1/2 * sin(\gamma_{[1]}) + \dot{\gamma}^2_{[1]} l1/2 * cos(\gamma_{[1]}))(j) \end{aligned} \tag{12}$$

$$\begin{aligned} a_{CM2} = (\ddot{x} + \ddot{\gamma}_{[1]} * l1 * cos(\gamma_{[1]}) + \dot{\gamma}^2_{[1]} * l2 * (-sin(\gamma_{[1]})))+ \\ +(\ddot{\gamma}_{[2]} * l2/2 * cos(\gamma_{[2]}) + \dot{\gamma}^2_{[2]} * l2/2 * (-sin(\gamma_{[2]})))(i)+ \\ +(\ddot{\gamma}_{[1]} * l1 * sin(\gamma_{[1]}) + \dot{\gamma}^2_{[1]} * l1 * cos(\gamma_{[1]}))+ \\ +\ddot{\gamma}_{[2]} * l2/2 * sin(\gamma_{[2]})) + (\dot{\gamma}^2_{[2]} * l2/2 * cos(\gamma_{[2]}))(j) \end{aligned} \tag{13}$$

Derivative of the Angular Momentum

The angular momentum for the planar motion, about the Z axis, through to the center of mass, is defined by:

$$H_{CM} = J_{CM} * \omega \tag{14}$$

J_{CM} refers to the moment of inertia of the body about the Z axis, normal to the plane and through the barycenter. The derivative is given by:

$$H'_{CM} = J_{CM} * \omega' \tag{15}$$

For both bars, we have:

$$J_{CM} = \frac{1}{12} * m * l^2(k) \tag{16}$$

$$H'_{CM1} = J_{CM1} * \ddot{\gamma}_{[1]}(k) \tag{17}$$

$$H'_{CM2} = J_{CM2} * \ddot{\gamma}_{[2]}(k) \tag{18}$$

External Actuation

The resultant force and torque aligned through the center of mass (wrench) must be determined for each body. Work done by internal forces and torques are null and will therefore not appear in the equations. The focus is on the external actuation.

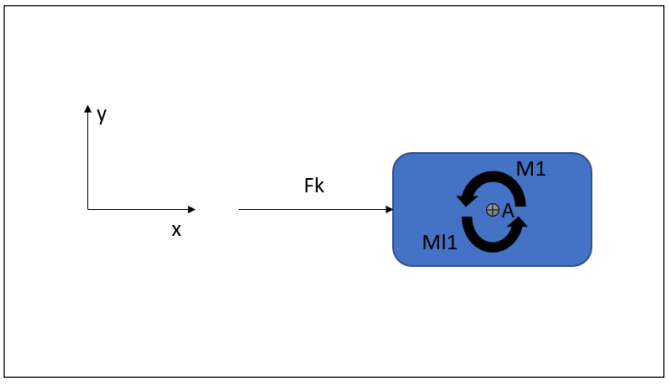

Figure 2: Free body diagram - Cart

From Figure 2, we can determine that the wrench on the center of mass of the cart is:

$$\begin{aligned} \sum F_x &= F_k \\ \sum F_y &= 0 \\ \sum M &= 0 \end{aligned} \tag{19}$$

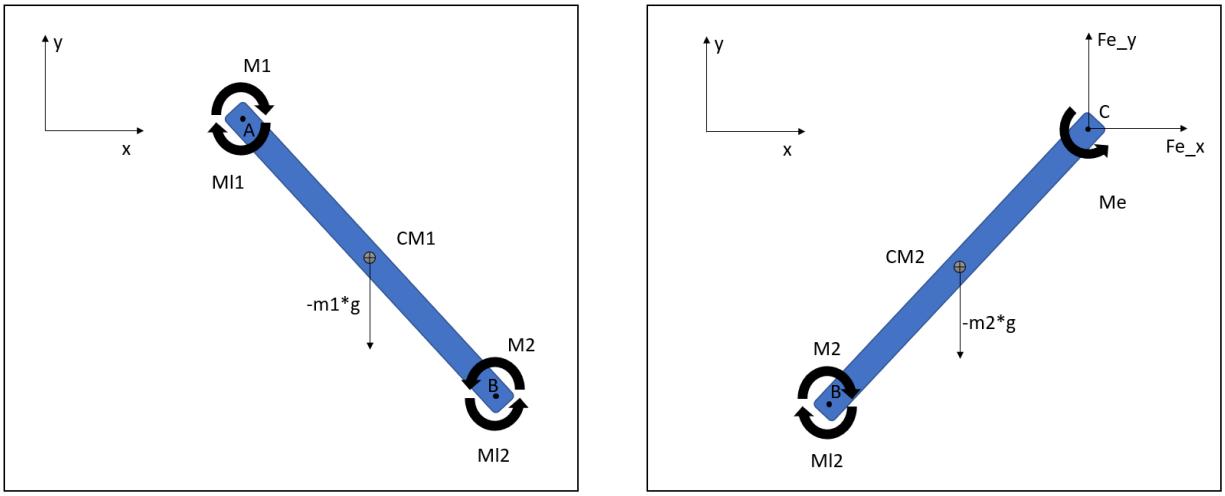

(a) First Bar

(b) Second Bar

Figure 3: Free body diagram

From figure 3a, we can determine that the wrench on the center of mass of the first bar is:

$$\begin{aligned} \sum F_x &= 0 \\ \sum F_y &= -m1 * g \\ \sum M &= M2 + Ml2 - M1 - Ml1 \end{aligned} \tag{20}$$

From figure 3b, we can determine that the wrench on the center of mass of the second bar is:

$$\begin{aligned} \sum F_x &= Fe_x \\ \sum F_y &= Fe_y - m2 * g \\ \sum M &= -M2 - Ml2 + Me + l2 * Fe_y * sin(\pi - \gamma_{[2]}) + l2 * Fe_x * sin(\frac{\pi}{2} - \gamma_{[2]}) \end{aligned} \tag{21}$$

After defining all these physical quantities, all the three equations of motion were implemented in Matlab. The integrator employed to solve the differential equations was the *ode45* in Matlab and a graphical interface was developed, see figure 5a.

DYNAMIC SIMULATION

To validate our model, a series of steps of increasing difficulty were taken, starting just from the equilibrium position with no springs, dampers or actuation, all the way to the combination of all. To perform the different simulations, different values were added to the system variables according to the desired dynamics. The most relevant steps are presented herein.

Damped Free Fall

In this case, dampers are added by changing the value of both damping coefficients (dampers of the rotational joints):

- $bl1 = 0 \rightarrow 0.7$; $bl2 = 0 \rightarrow 0.7[\frac{N*m*s}{rad}]$

The results of this simulation are shown in figure 4a. As expected, the damping resulted in the system converging to the equilibrium position pointing down.

All Parameters

A simulation with all the parameters set is presented; parameter values are set as:

- $bl1 = 0 \rightarrow 5$; $bl2 = 0 \rightarrow 5[\frac{N*m*s}{rad}]$
- $kl1 = 0 \rightarrow 40$; $kl2 = 0 \rightarrow 20[\frac{N*m}{rad}]$

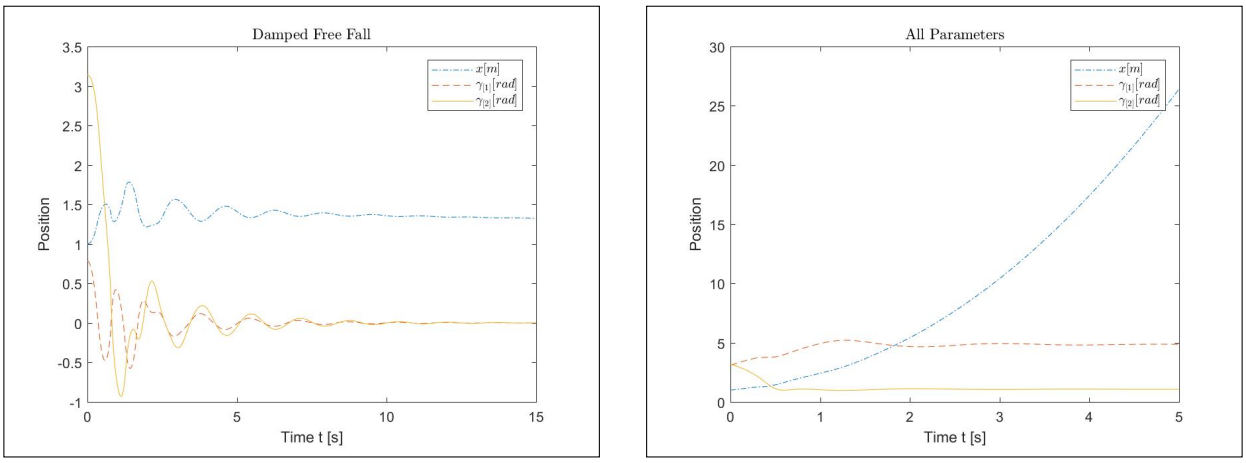

(a) Simulation Results - Damped Free Fall

(b) Simulation Results - All Parameters

Figure 4: Model and Simulation

- $M1 = 0 \rightarrow -15$; $M2 = 0 \rightarrow 15[N*m]$
- $Me = 0 \rightarrow 15[N*m]$
- $Fe_x = 0 \rightarrow 10$; $Fe_y = 0 \rightarrow -30[N]$

Initial position:

$$Y_0 = [1, \pi, \pi, 0, 0, 0]' \tag{22}$$

The simulation results are presented in figure 4b. The most important aspect is the fact that, due to the absence of springs and stops on the cart, Fe_x keeps on increasing the speed of the system. Coordinate x tends to infinity if this actuation is maintained. Other aspects, such as motor and springs behavior, also match the expected dynamics.

INVERSE DYNAMICS

In this section, the equations of motion are used to find the necessary forces to perform a desired movement.

The chosen kinematics is: the end-effector has to follow a circular path at constant speed. The end-effector must be at a constant inclination:

- Simulation 1 - $\gamma_{[2]} = \frac{\pi}{4}$; Simulation 2 - $\gamma_{[2]} = \frac{3\pi}{4}$

The circular trajectory will be defined by:

- Simulation 1 - $Radius = 0.5[m]$; $Center = [1 + \frac{\sqrt{2}}{2}, \frac{\sqrt{2}}{2}]$; Simulation 2 - $Radius = 0.5[m]$; $Center = [1 + \frac{\sqrt{2}}{2}, \frac{-\sqrt{2}}{2}]$

The trajectories can be seen in red in figure 5a. The angle in the red circle varies with time (t).

From figure 5b, we can obtain $x(t)$ and $\gamma_{[1]}(t)$. The result is:

$$\begin{aligned} \gamma_{[1]}(t) &= arcsin(\frac{R}{l1} * sin(t*\omega)) + \frac{\pi}{2} \\ x(t) &= C1 + R*cos(t*\omega) - l1*cos(\gamma_{[1]}(t) - \frac{\pi}{2}) \end{aligned} \tag{23}$$

The first and second derivatives $\dot{\gamma}_{[2]}$ and $\ddot{\gamma}_{[2]}$ are 0, the first and second derivatives for $x(t)$ and $\gamma_{[1]}(t)$ are calculated from the equations above.

The next step is to manipulate the dynamics equations to isolate Fk, $M1$ and $M2$ (force on the cart and two motors located on the rotational joints). Substituting $\gamma_{[2]}$, $x(t)$, $\gamma_{[1]}(t)$, and its derivatives in these equations results in expressions for the force and torques: $Fk = f1(t)$, $M1 = f2(t)$ and $M2 = f3(t)$.

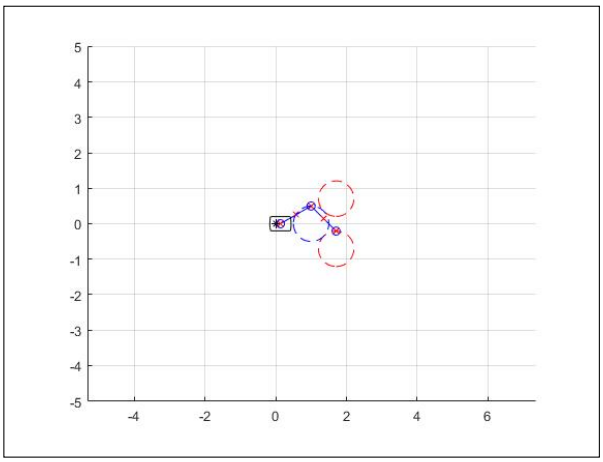

(a) Desired Trajectory

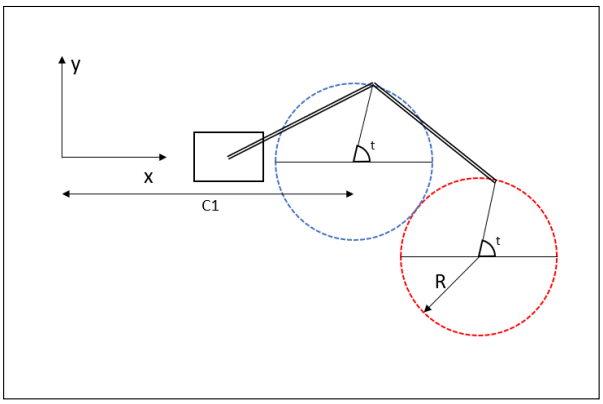

(b) Detail - Kinematic

Figure 5: Trajectory

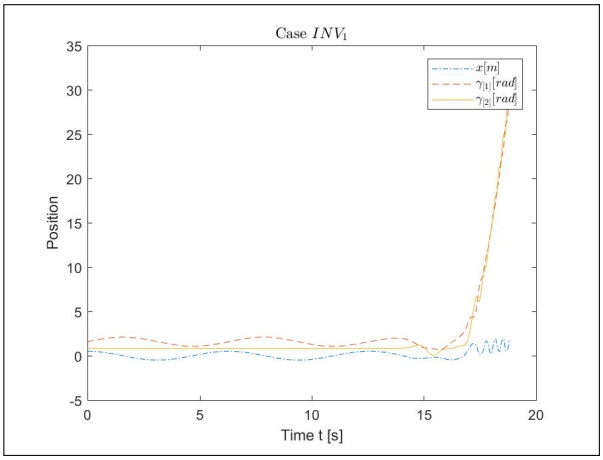

(a) Simulation 1 Results - Inverse Dynamics

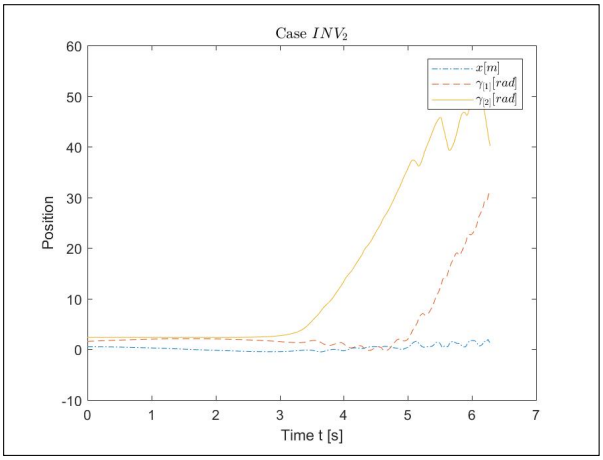

(b) Simulation 2 Results - Inverse Dynamics

Figure 6: Simulations

Simulation 1

Figure 6a shows the result of the first simulation. We can observe that up to 15 seconds, the system practically follows the desired trajectory. Yet the numerical errors start to accumulate, resulting in a chaotic behavior after that. The numerical errors are amplified because, during the motion, the mechanism almost reaches a singular configuration, fully extending its "arm", $\gamma_{[1]}$ gets close to $\gamma_{[2]}$.

In real life, we do not have numerical errors, but we do have mechanical imperfections, perturbation and imperfect actuation. These problems would be more than enough to destabilize a system that has no feedback control.

Simulation 2

Figure 6b depicts the result of the second simulation. For the second trajectory, the system reaches a chaotic state much faster. Even though the feed-forward of the system dynamics is a very powerful tool, it is most effective when combined with adequate control.

LINEAR QUADRATIC REGULATOR - INVERTED PENDULUM

The last part of this paper consists in the control implementation. Now, the system is treated as a double inverted pendulum, and our goal is to stabilize it vertically at a desired position x. All the external actuation forces, springs and dampers were removed from the system, with one exception: Fk, which is now going to be controlled through full state feedback.

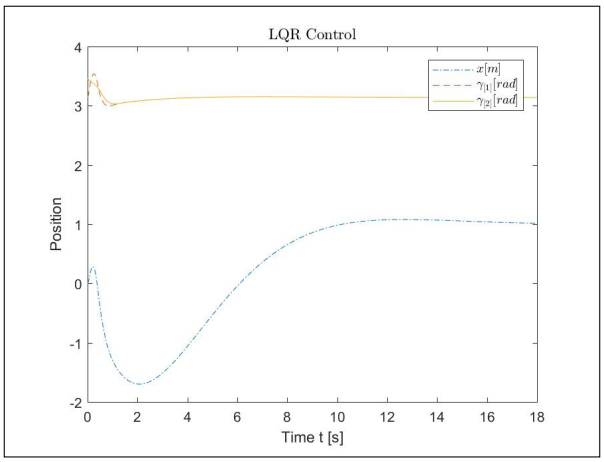

Figure 7: Simulation Results - LQR Control

The linear quadratic regulator (LQR) is an optimal control strategy, and has reasonable performance when dealing with this type of problem (Mohan and Singh, 2013; Varghese et al., 2017). LQR was implemented in Matlab by first linearizing the system, then choosing a matrix Q as $C * C'$ (C being the controllability matrix) and R as 1 (since we only have one actuator).The result is the gain matrix as follows

$$K = \begin{bmatrix} 1 & 320.59 & -347.43 & 4.05 & 6.75 & -54.07 \end{bmatrix} \tag{24}$$

To implement the control, Fk is defined as $-K * [Y - X_d]$, where X_d is the vector of the desired values for the state: $X_d = [1, \pi, \pi, 0, 0, 0]'$. The simulation results can be observed in Figure 7.

CONCLUSIONS

The double pendulum on a kart is an extremely chaotic, nonlinear and coupled system. All the simulations and tests provided some evidence that the dynamic equations representing the system were correctly implemented. The Gibbs-Appell method was proven to be convenient for modeling the dynamics of the approached planar mechanism, especially due to its versatility for dealing with multi-body systems. The results herein encourage us to apply the Gibbs-Appell method to more complex mechanisms.

REFERENCES

Baruh, H., 1999, "Analytical dynamics", WCB/McGraw-Hill.

Desloge, E. A., 1988, "The Gibbs-Appell equations of motion", American Journal of Physics, 56(9):841-846.

Kane, T. R. and Levinson, D. A., 1985, "Dynamics, theory and applications", McGraw-Hill.

Li, L., Jiang, S., Dai, F., and Gao, X., 2014, "Dynamic model and balance control of two-wheeled robot with non-holonomic constraints", in Proceeding of the 11th World Congress on Intelligent Control and Automation, pages 503-508, IEEE.

Matarazzo Orsino, R. M. and Hess-Coelho, T. A., 2015, "A contribution on the modular modelling of multibody systems", Proceedings of the Royal Society A: Mathematical, Physical and Engineering Science, 471(2183):20150080.

Mohan, V. and Singh, N., 2013, "Performance comparison of LQR and ANFIS controller for stabilizing double inverted pendulum system", in 2013 IEEE International Conference on Signal Processing, Computing and Control (ISPCC), pages 1-6, IEEE.

Varghese, E. S., Vincent, A. K., and Bagyaveereswaran, V., 2017, "Optimal control of inverted pendulum system using PID controller, LQR and MPC", IOP Conference Series: Materials Science and Engineering, 263(5):052007.

Wang, L.-S. and Pao, Y.-H., 2003, "Jourdain's variational equation and Appell's equation of motion for nonholonomic dynamical systems", American Journal of Physics, 71(1):72-82.